Electronic Supplementary Material (ESI) for Journal of Materials Chemistry C.

Supporting Information

Effects of PNDIT2 end groups on aggregation, thin film structure, alignment and electron transport in field-effect transistors

Rukiya Matsidik,[a,b] Alessandro Luzio,[c] Sophie Hameury [a], Hartmut Komber[d], Christopher R. McNeill[e], Mario Caironi[c] and Michael Sommer [a,b,f]

[a]Universität Freiburg, Makromolekulare Chemie, Stefan-Meier-Str. 31, 79104 Freiburg, Germany

[b]Freiburger Materialforschungszentrum, Stefan-Meier-Str. 21, Universität Freiburg, 79104 Freiburg, Germany

[c]Center for Nanoscience and Technology @PoliMi, Instituto Italiano di Tecnologia, Via Pascoli 70/3, 20133 Milano, Italy

[d]Leibniz Institut für Polymerforschung Dresden e.V., Hohe Straße 6, 01069 Dresden, Germany

[e]Department of Materials Engineering, Monash University, Clayton, Victoria 3800, Australia

[f]Freiburger Institut für interactive Materialien und bioinspirierte Technologien, Georges-Köhler Allee 105, 79110 Freiburg

Content

1. Additional UV-vis spectra

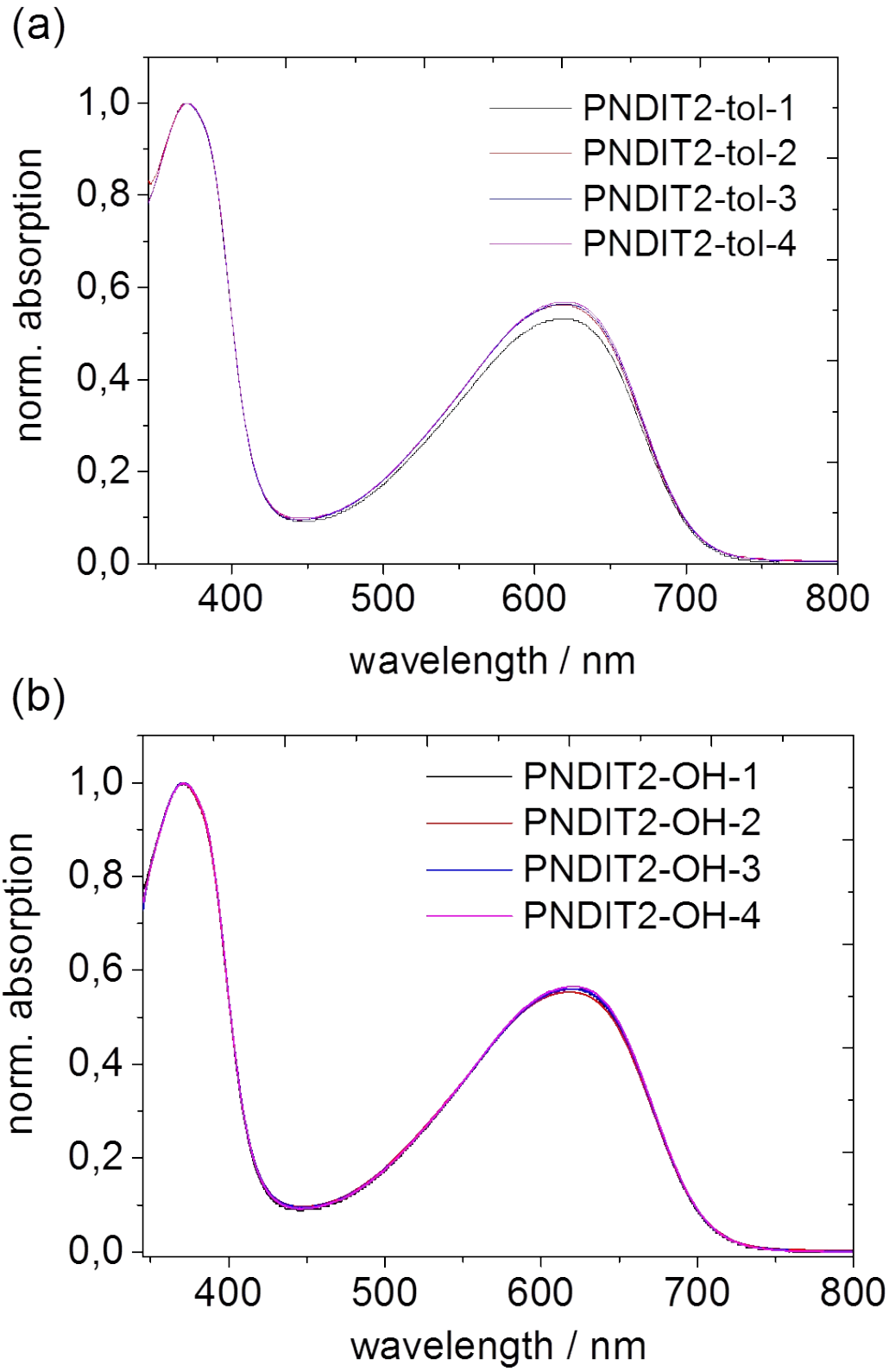

Figure S1. UV-vis absorption spectra of (a) PNDIT2 made in toluene and (b) made in 2-MeTHF with varying MW at RT in 1-chloronaphthalene

2. Thermal characterization

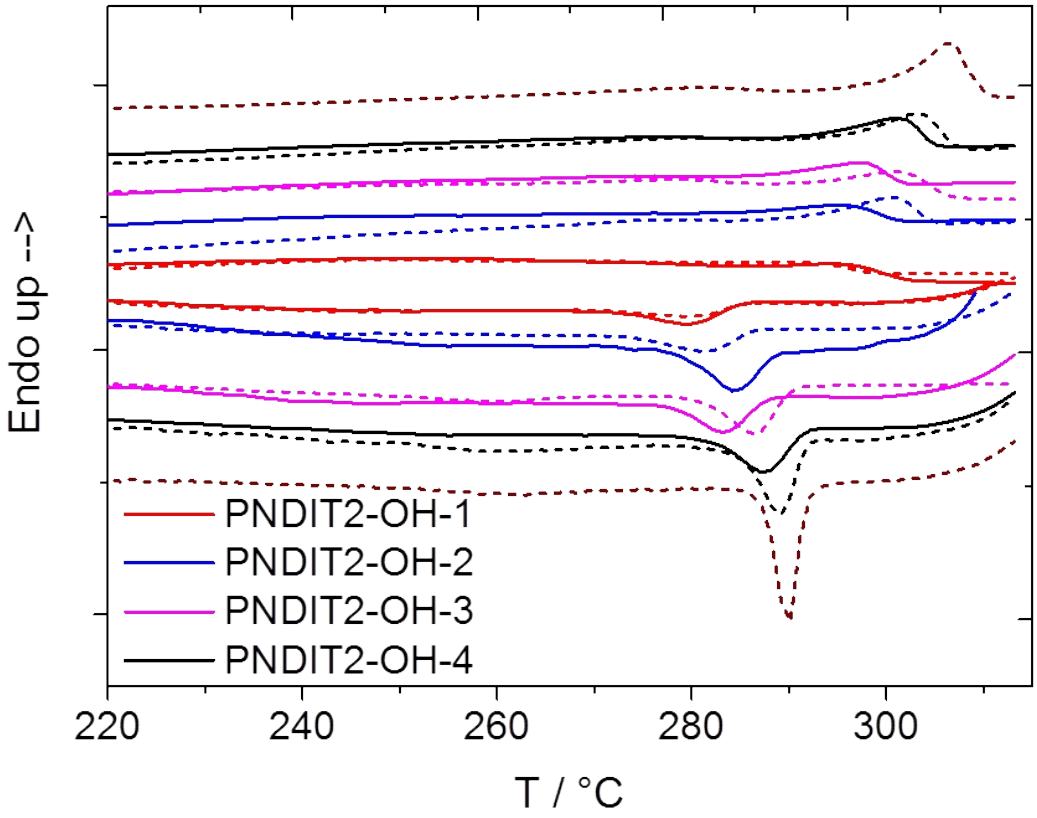

Figure S2 DCS curves of PNDIT2 samples with increased molecular weight. Dash line: reference samples made in toluene (table 2); Solid line: samples made in MeTHF

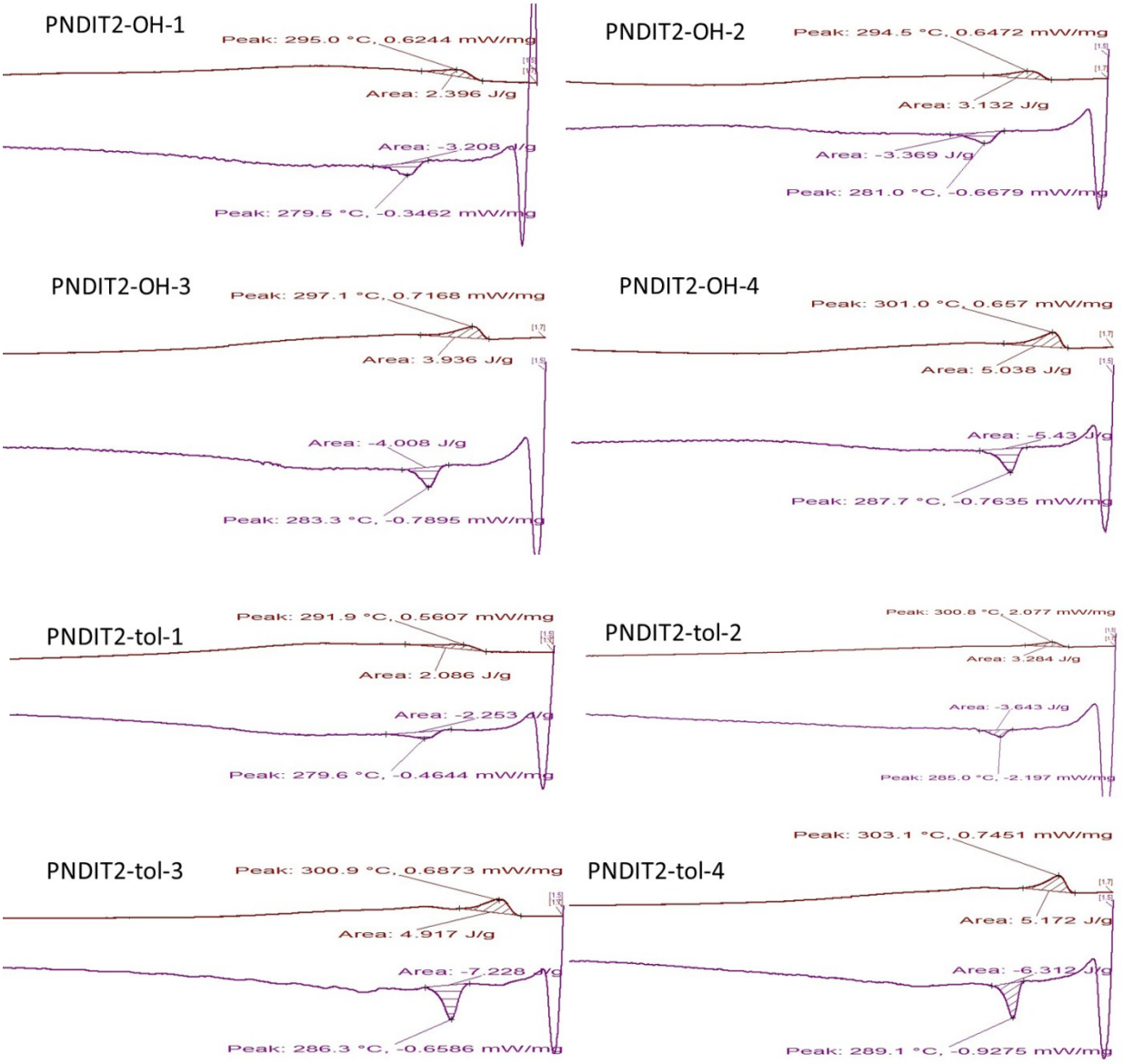

Figure S3 Evaluation of melting and crystallization temperatures and enthalpies of samples from Figure S2

3. ^{1}H NMR spectra

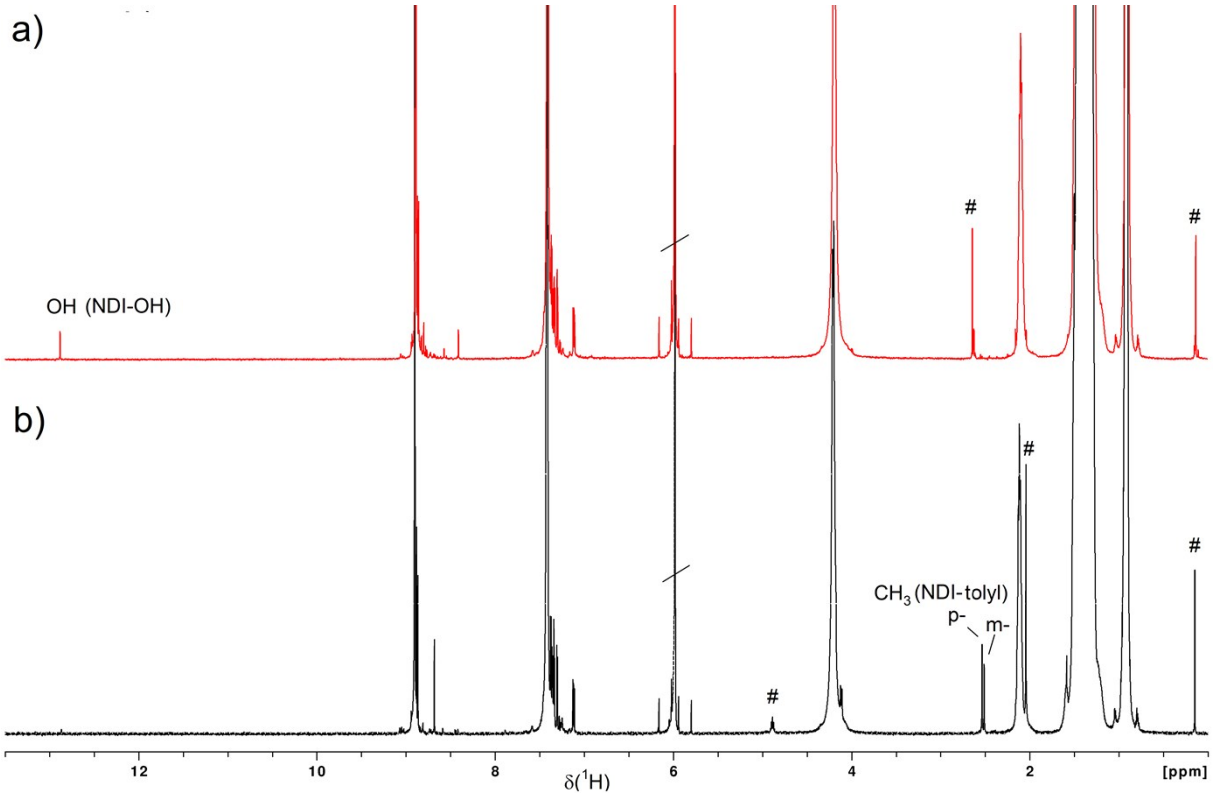

Figure S4. Full ^{1}H NMR spectra of PNDIT2 (a) made in MeTHF (entry 25) and (b) reference PNDIT2 made in tol (PNDIT2 tol-4). The spectra are enlarged for better visibility of end group signals. In addition to the signals assigned in Figure 3, the OH signal of the NDI-OH end group (a) and the methyl signals of the isomeric NDI-tolyl end groups (b) are assigned (cf. R. Matsidik, H. Komber and M. Sommer, *ACS Macro Lett*., **2015**, *4*, 1346–1350). # marks signals of impurities. Spectra were measured at 120 °C in $C_2D_2Cl_4$.

4. Additional AFM images

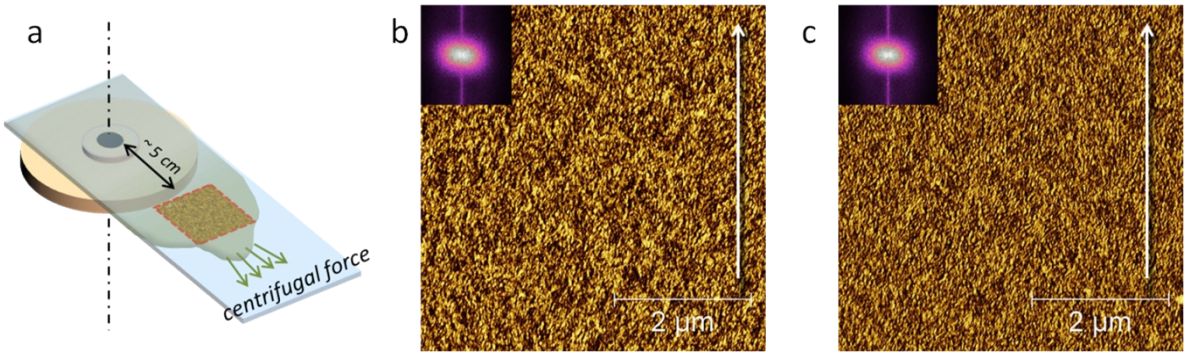

Figure S5 (a) Schematic of spin coating off-centre deposition: film topography is checked at a distance of ~ 5 cm from the centre of the spin, where the flow is dominated by centrifugal force field; AFM topography images of PNDIT2-tol-4 (b) PNDIT2-OH-4 (c) deposited from toluene using off-centre spin coating; domains directionality is highlighted through 2D Fast Fourier Transform (FFT) images (insets) extracted from the same AFM images; centrifugal forces direction is also indicated (white arrows).

5. Additional OFET characterization

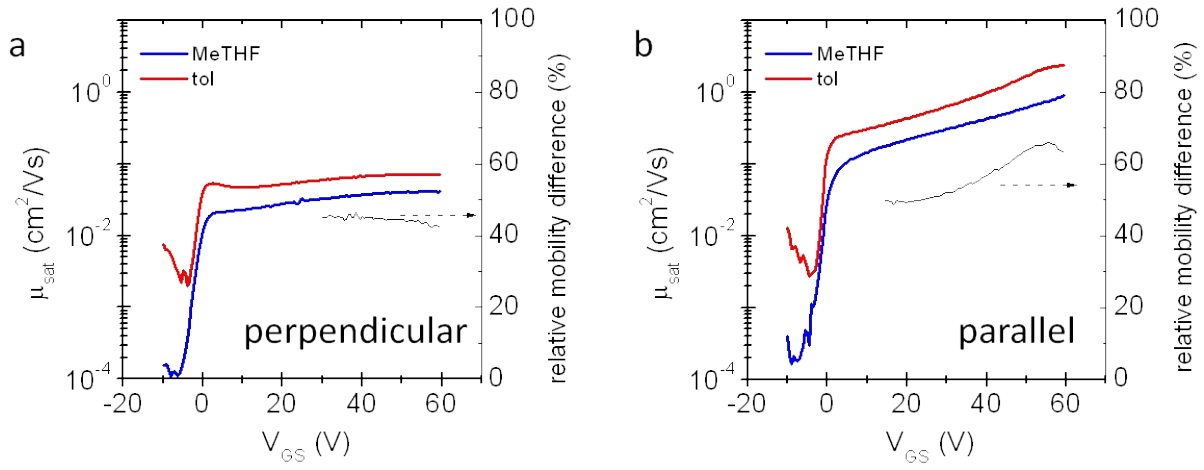

Figure S6 plots of saturation mobility (μ_{sat}) as a function of the applied gate bias (V_{GS}) for off-centre spin coated films, in case of transport parallel (a) and perpendicular (b) to the backbones/fibrils direction; the relative difference of mobility between the batch from MeTHF and the batch from toluene is also reported.

6. 2D GIWAXS images

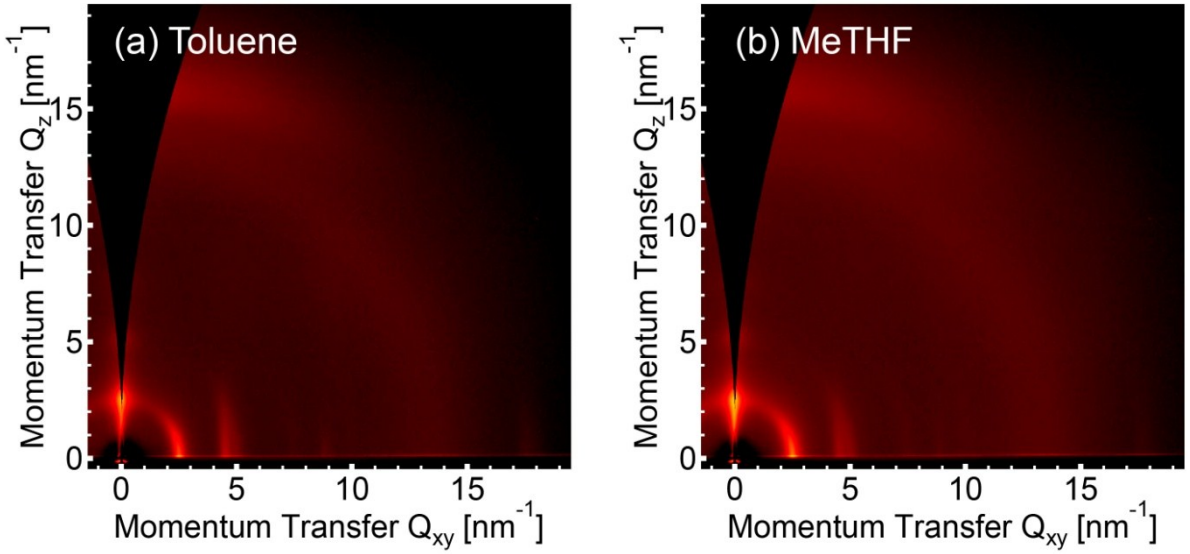

Figure S7 2D GIWAXS images taken of the (a) toluene sample and the (b) MeTHF sample spin-coated from DCB.